Uncertainties in risk assessment of hydrogen discharges from pressurized storage vessels at low temperatures

Markert, Frank; Melideo, D.; Baraldi, D.

Published in:
Proceedings of 5th International Conference on Hydrogen Safety

Publication date:
2013

UNCERTAINTIES IN RISK ASSESSMENT OF HYDROGEN DISCHARGES FROM PRESSURIZED STORAGE VESSELS AT LOW TEMPERATURES

Markert, F.[1], Melideo, D.[2] and Baraldi, D.[2]
[1] Department of Management Engineering, Technical University of Denmark, Produktionstorvet 424, Kongens Lyngby, 2800, Denmark, fram@dtu.dk
[2] Institute for Energy and Transport, Joint Research Centre European Commission, Westerduingweg 3, Post box 2, Petten, 1755 ZG, Netherlands, daniele.melideo@ec.europa.eu, daniele.baraldi@jrc.nl

ABSTRACT

Evaluations of the uncertainties resulting from risk assessment tools to predict releases from the various hydrogen storage types are important to support risk informed safety management. The tools have to predict releases from a wide range of storage pressures (up to 80 MPa) and temperatures (at 20K) e.g. the cryogenic compressed gas storage covers pressures up to 35 MPa and temperatures between 33K and 338 K. Accurate calculations of high pressure releases require real gas EOS. This paper compares a number of EOS to predict hydrogen properties typical in different storage types. The vessel dynamics are modeled to evaluate the performance of various EOS to predict exit pressures and temperatures. The results are compared to experimental data and results from CFD calculations.

1.0 INTRODUCTION

Hydrogen may be thermodynamically considered as an almost ideal gas over a very wide temperature and pressure range. Nevertheless, present technological developments stores hydrogen in the liquid state at about 20K under a low pressure of few bars and in the gaseous state at very high pressures up to 800 – 1000 bars at ambient temperatures. Recently, the operational regime of cryo compressed hydrogen (CcH2) storage was reported to cover pressures of up to 35 MPa and temperatures from +65 °C down to -240 °C [1,2]. Considering these wide ranges for temperature and pressures, the assumption of ideal gas behavior and application of the ideal gas equations of state (EOS) is not adequate for all situations. This has been recognized by the scientific community and different approaches describing high pressure gas releases at ambient conditions from storage tanks [3-7] and within vehicles [8] are described. This discrepancy of behavior between ideal gas and real gas is illustrated in Figure 1, where the state-of-the-art reference data provided by NIST[1] [3] are compared against predictions using the EOS for ideal gas. It is shown that the ideal gas EOS accuracy in predicting the density pressure relationship is limited up to about 35MPa at 500K, and up to about 15MPa at 200K.

From the risk assessment point of view a large number of release scenarios have to be analyzed, to give a comprehensive evaluation of the associated risks and to provide useful data for risk management purposes. In many scenarios at ambient conditions and moderate storage pressures the use of engineering equations based on the ideal gas EOS may give sufficiently accurate results to make proper decisions. For scenarios using very high pressure and cryogenic storage real gas behavior needs to be taken into account to reduce the level of uncertainty in the evaluations. For this purpose several EOS are being developed which may be classified into the cubic EOS type[2] (equations by e.g.

[1] Accesible from http://webbook.nist.gov/chemistry/fluid "hydrogen" and described in the PhD thesis by Leachman: http://www.boulder.nist.gov/div838/theory/refprop/leachman.pdf
[2] http://en.wikipedia.org/wiki/Equation_of_state#Cubic_equations_of_state

Abel-Nobel[3]; van-der-Waals; Redlich-Kwong; Redlich-Kwong-Soave; Peng-Robinson; Beatty-Bridgeman) using corrections for the gas volume and pressure assuming the finite volume of the

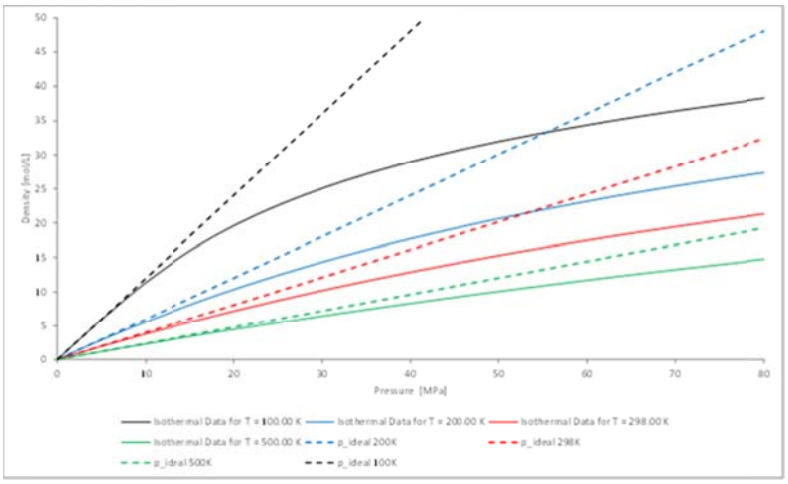

Figure 1. Real gas behaviour for some isotherms (continuous line) compared to ideal gas behaviour (dotted lines).

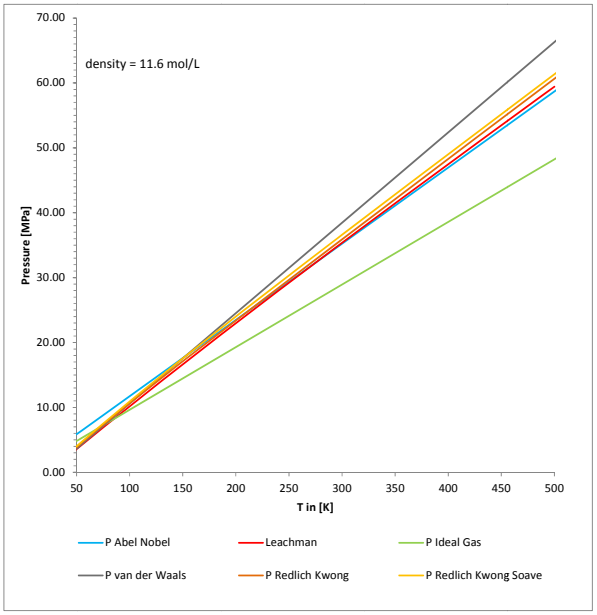

Figure 2. Isochoric temperature –pressure plots for 11.6 mol/L (equal to about 35MPa at ambient temperature) showing the accuracy of some cubic EOS compared to the NIST data and the ideal EOS

molecules and the intermolecular forces, respectively. The accuracy of these to predict the temperature- pressure behavior at constant density of 11.6 mol/L, which is the density of hydrogen in a 35 MPa pressurized storage at ambient temperatures, is illustrated in Figure 2. Recently, eleven expressions of the cubic EOS family have been reviewed on their accuracy predicting various supercritical properties of hydrogen by Nasrifar [9].

The authors are not aware of release experiments in the low temperature range, but with the findings described above, it is important to address such releases. This paper is a first theoretical analysis to identify the potential uncertainty in the predictions of hydrogen releases at low temperatures and to

[3] The Abel-Nobel EOS only assumes corrections to the finite volume of the molecules

evaluate the possible effects to overall hydrogen safety using the correlations on jet flame length by Saffers and Molkov [10] and correlations on explosion severity by Dorofeev [11].

2.0 THEORETICAL BACKGROUND

For risk assessment purposes, it may be sufficient to know the initial vessel conditions using the initial mass release to take a conservative approach, as the initial value is the maximum during the whole release process. In the case, where more detailed release scenarios are required, a time dependent approach has to be taken into account to predict mass release rate decays. Hereunder, it is important to know about parameters like vessel temperature, vessel pressure, throat pressure and sonic speed of the released gas that determine jet properties and jet flames. Therefore, models need to be capable of predicting such parameters. This paper will focus on the accuracy to model time dependent vessel pressures and temperatures and mass release.

Several EOS are applied to calculate the mass release rate at ambient (300 K) and low (200 K) temperatures at two vessel pressures (30 and 34.5 MPa). The implementation of the real gas properties is implemented using the compressibility factor Z (see appendix A). The temperature profile in the vessel as well as important release parameters are calculated using an engineering numerical model called “DTU analytical model” in the following. It is developed to predict vessel dynamics and it is based on a model description from the Yellow book (see appendix A and CPR 14E chapter 2.5.2.2; [12]) and a CFD model [7] using on the one side the ideal gas EOS and selected cubic EOS. The results are compared to former findings by Mohamed and Paraschivoiu [13].

There are a great number of articles describing pressurized releases at ambient temperatures at moderate pressures. In such scenarios the specific heat ratio C_p/C_v is only slightly dependent on temperature and pressure as shown in Figure 3 for 298 and 500K. At low temperature an increasingly stronger dependency on pressure is observed for C_p/C_v which is illustrated in Figure 3. Also, the decay of the isochoric heat capacity C_v is shown. As the dependency of C_v is close to linear, it is obvious that the pressure dependency for C_p is becoming strongly non-linear at low temperatures.

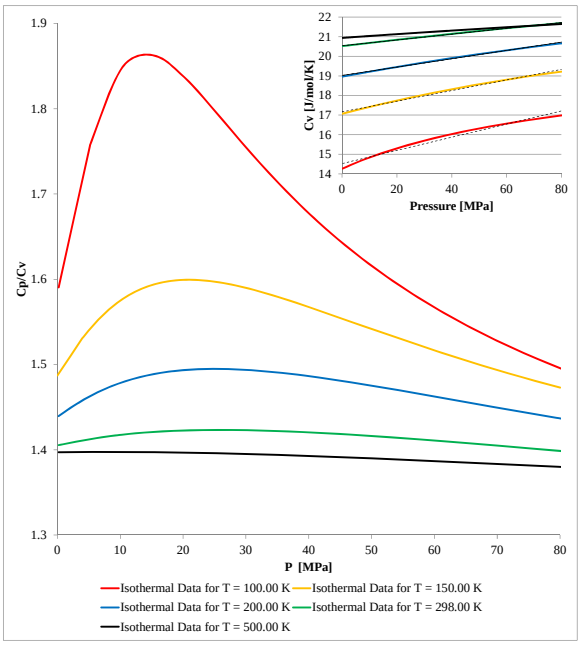

Figure 3. Real gas behaviour of normal hydrogen: C_p/C_v vs. pressure at several isotherms. Also shown (small figure) C_v versus pressure at the same isotherms. The dotted lines are linear fits to the graph and the respective coefficients are listed in Table 1

Isochoric data for the temperature dependency of C_p and C_v are shown for densities from 2 – 21.3 mol/L in Figure 4. It is seen that C_v values are only slightly dependent on pressure. Therefore, the DTU analytical model predicts the temperature variation of C_v using a fit to the original data at a low density in a limited temperature interval relevant for the calculations. The C_p (2mol/L) curve follows the shape of the C_v curves real gas behavior shows a strong increase in C_p at low temperatures with little difference comparing densities at 21.3, 20.4 and 11.6 mol/L.

Being a diatomic linear molecule, hydrogen has three translational and two rotational degrees of freedom contributing to its specific heat capacity. Thus, hydrogen's theoretical predicted specific heat capacity C_v is close to 3.5R= 20.785 J $mol^{-1}K^{-1}$, as it is actually observed at 500 K and 298 K with 20.953 and 20.47 J $mol^{-1}K^{-1}$, respectively. With decreasing temperatures the specific heat capacity C_v is falling approaching the theoretical value for monatomic gases (three degrees of freedom) of 1.5R= 12.471 J $mol^{-1}K^{-1}$. Thus, at low temperatures, hydrogen is thermodynamically behaving as a monatomic gas, which is caused by quantum effects reducing the number of possible rotational energy levels. The rotational energy level gap is getting much larger than kT[4] at 60 K[5)] and, by that, the two rotational energy levels are decreasingly less populated with decreasing low temperatures. The onset temperature for this quantum effect is T< 160K according to [9]. Additional findings and references may be found in [14].

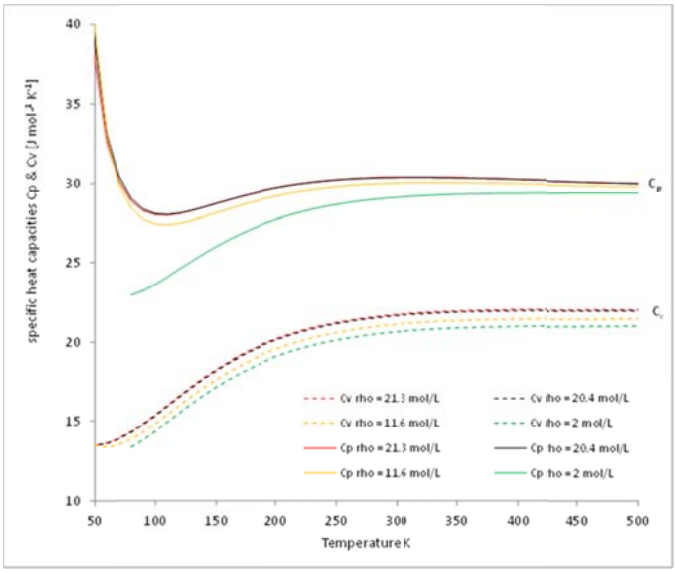

Figure 4. Isochoric data for the temperature dependency of C_p and C_v are shown for densities, rho=2 - 21.3 mol/L.

Table 1. Linear fit to C_v plots in Figure 3 (shown there as dotted lines)

T K	C_v-slope	C_v ideal	R^2
500	0.0088	20.953	0.9992
298	0.0152	20.47	0.9984
200	0.0213	19.023	0.9966
150	0.0271	17.165	0.9926
100	0.0336	14.525	0.9756

[4] kT is an energy level with k being the Boltzmann constant and T the absolute temperature
[5] Chapter 8; Heat capacity and the expansion of gases (page 5) orca.phys.uvic.ca/~tatum/thermod/thermod08.pdf

3.0 THE CASE STUDY

3.1 Engineering modeling strategy

The following scenarios are used to compare the DTU analytical model with the JRC CFD release model. For validation purposes, the first scenario is equal to the configuration in Mohamed and Paraschivoiu's paper [13]. The release is from a hole r=3.18mm in a 27 L cylindrical tank. The initial tank pressure is 34.5 MPa at a temperature of 300 K. Mohamed and Paraschivoiu used the Beattie-Bridgeman EOS and a 3-D unstructured tetrahedral finite volume Euler solver to model a high pressure hydrogen release at ambient temperature. They additionally applied an analytical model with the following assumptions: the thermodynamic properties are uniform in the tank; the release occurs at adiabatic conditions; the release is sonic at the orifice (velocity of gas is equal to the local speed of sound); the expansion of hydrogen from the stagnation state in the vessel to the critical state at the orifice takes place in a small region near the orifice being modeled as quasi one-dimensional isentropic flow. These assumptions for the analytical model are essentially the same as used in the DTU analytical model.

In the second scenario, the geometry is kept unchanged while the initial pressure and temperature are equal to 30 MPa and 200 K respectively. In the third scenario, a much larger tank was considered (197 L and 5.7 mm orifice radius) with the same initial conditions like in case 2.

3.2 CFD modeling strategy

The ANSYS CFX14.0 fully compressible solver was used [15]. Hybrid axy-simmetric meshes were generated with Pointwise 17.0 [16]as shown in Figure 5. The mesh is a pseudo 2-dimensional mesh since it is one cell thick in the y direction and it represents 1/360 of the whole 3D geometry. The main domain in the tank is built with an unstructured tetrahedral mesh. Since in the leak a preferential direction in the movement of the flow can be easily identified, a structured mesh was generated in that region. In the validation case with the 27 L tank, two computational grids were built in order to investigate the

Table 2. Selected scenarios

	Tank volume (L)	Orifice diameter(mm)	Initial pressure(Mpa)	Initial temperature(K)
case 1 (Validation)	27	3.18	34.5	300
case 2	27	3.18	30	200
case 3	197	5.7	30	200

grid independence. The number of nodes in the meshes is reported in Table 3. It must be emphasized that the number of nodes is reported instead than the number of cells because in ANSYS-CFX the control volumes are built around the nodes and therefore their number is equal to the number of nodes. Negligible differences were observed in the results between the two grids. The high resolution advection scheme and the second order backward Euler time scheme were selected. The free slip boundary condition is applied to the walls and the exit surface is modeled as a supersonic outlet boundary condition, following the modeling strategy by Mohamed and Paraschivoiu [13].

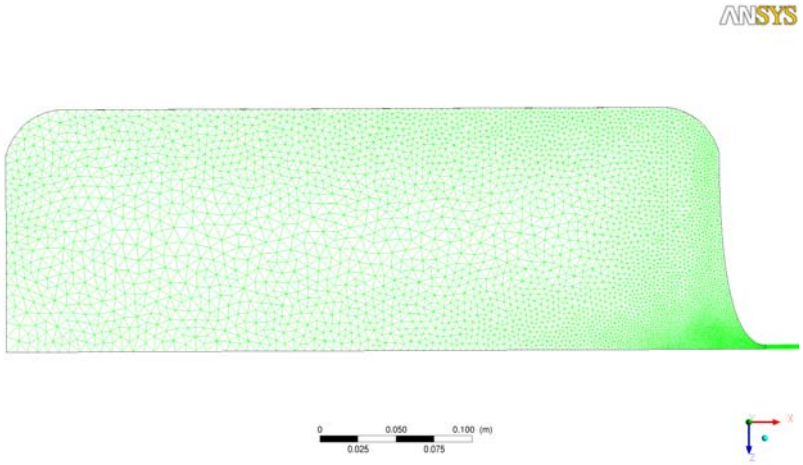

Figure 5: Computational mesh.

Table 3: Number of nodes in the computational grids.

Mesh	Number of nodes
27 L coarse	2984
27 L fine	13380
200 L	7328

4.0 RESULTS

4.1 Case 1: 27L vessel at ambient conditions

Simulations are performed for the ideal gas release, the CFD code using the Peng Robionson EOS and the engineering model using Leachman's EOS adaption for the compressible factore Z [3,17]. In the engineering model, the specific heats are variated: 1) Cv and Cp taken as constant at initial vessel temperature; 2) Cv and Cp taken as constant at (Tend-Tstart)/2 and finally 3) as a function of the temperature Cv(T) and Cp (T). Furthermore, the results are compared to the one's published by Mohamed et al. [13] using an analytical and a 3D CFD approach.

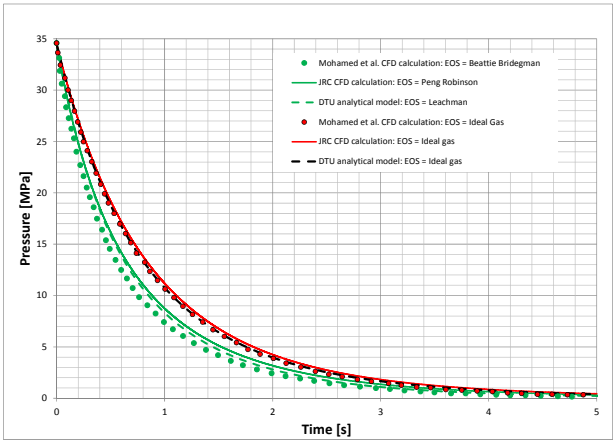

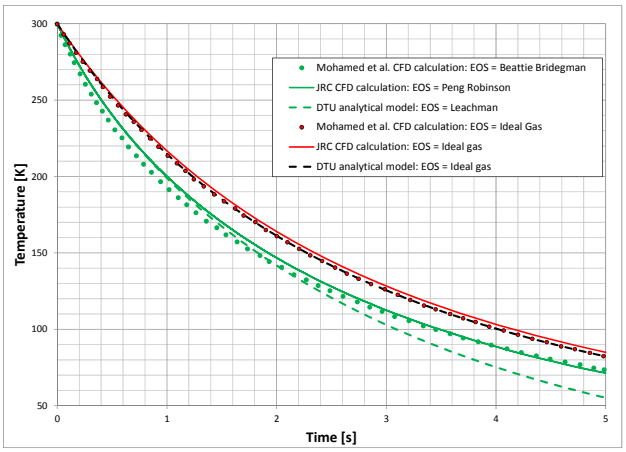

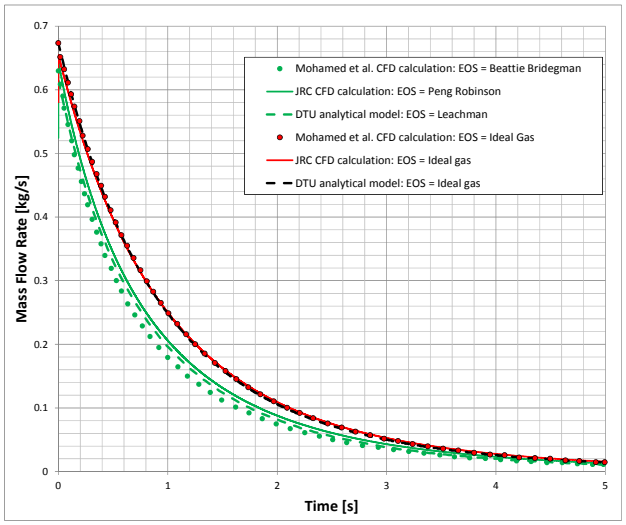

Figure 6. Release calculations at 300K and a vessel pressure of 34.5MPa. The hole-radius is 3.18mm. The JRC CFD calculation and the DTU analytical model are compared with the CFD calculations by Mohamed et al..

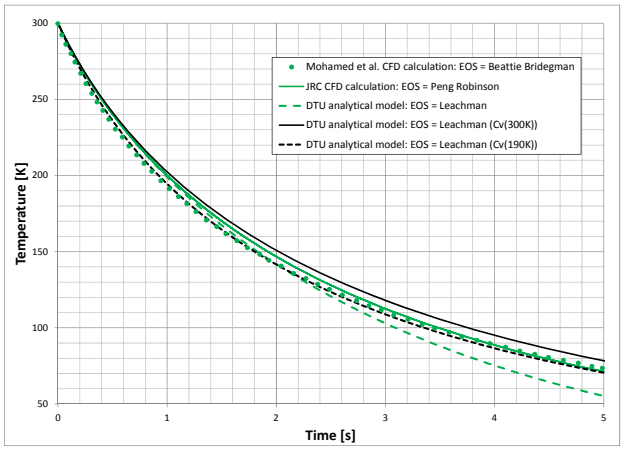

Figure 7.Time profiles of the vessel temperature using Beattie Bridgeman (Mohamed et al.), Peng Robinson (JRC CFD) and Leachman (DTU analytical model). In the latter C_v values are: a) function of temperature, b)constant value C_v at 300K (solid black line) and c) constant value C_v at 190K (T_{end}-T_{start})/2; dotted black line).

At ambient conditions all the models with the different real gas EOS provide very similar results. It is valid for the mass flow decay, the pressure decay in the vessel as well as the temperature decay in the vessel. The ideal gas approach is providing conservative release duration, while the initial releases are about the same for all.

4.2 Case 2: 27L vessel at low temperature

Simulations are carried out for the ideal gas release, the CFD code using the Peng Robionson EOS and the engineering model using Leachman's EOS adaption for the compressible factor Z [3,17]. The specific heats are varied: 1) C_v and C_p taken as constant at initial vessel temperature; 2) C_v and C_p taken as constant at $(T_{end}-T_{start})/2$ and finally 3) as a function of the temperature $C_v(T)$ and C_p (T).

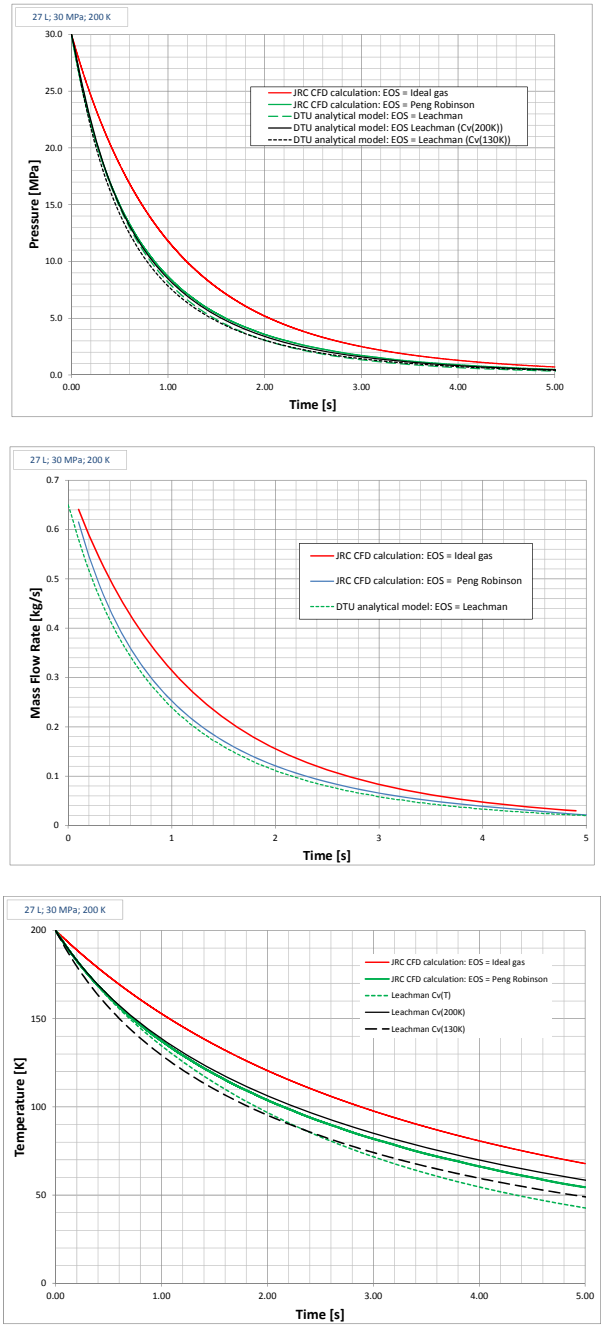

Figure 8. Results from the 27L storage release hole radius 3.18mm at 34.5 MPa at 200 K storage temperature.

In Figure 8 the results for the mass release shows the highest release for the ideal gas approximation being thus a conservative approach. The initial rates are about the same for all simulations. The models using the real gas predictions give about the same results. Similar findings are valid for the vessel pressure time profile. The temperature of the gas in the vessel is predicted considerably different comparing the three EOS applied. It further shows that the approximation of Cv and Cp/Cv is important to chose as some differences are observed. Due to the lack of experimental data it is not possible to predict the real temperature decay and giving recommendations on the best approach for predictions. The sound velocity has been calculated as seen in Figure 8.

4.3 Case 3: 200L vessel at low temperature

In order to test the basic assumptions made for the engineering model, as e.g. homogeneous pressure and temperature distribution inside the tank the following tests with a 200L vessel are performed using the CFD code from JRC and the engineering model adapted from the yellow book. The hole size radius is 5.7mm and the hydrogen is stored at 30 MPa at 200K.

Simulations are made for the ideal gas release, the CFD code using the Peng Robinson EOS and the engineering model using Leachman's EOS adaption for the compressible factor Z [3,17]. The specific heats are varied: 1) C_v and C_p taken as constant at initial vessel temperature; 2) C_v and C_p taken as constant at $(T_{end}-T_{start})/2$ and finally 3) as a function of the temperature $C_v(T)$ C_p (T).

The results are shown in Figure 9 for the mass release shows good comparison for the mass flow time dependency though the initial rate for the engineering model is slightly decreased. The decay curve though is close to the one obtained by the Peng Robinson CFD modeling approach. There are larger differences in the temperature decay, while the pressure decays are in excellent agreement.

4.4 Accident consequence

In the case of ignition, a hydrogen release can develop into a jet fires or an explosion depending on the local conditions and on the position and time of ignition. The consequences of those scenarios can be evaluated with simple methods.

An indication on the flame length can be provided by the correlation by Saffers and Molkov [18]. For under-expanded jets like in the case that is investigated in this paper, they developed the following correlation:

$$\frac{L_F}{D} = 805\left[\frac{\rho_N}{\rho_S}\left(\frac{U_N}{C_N}\right)^3\right]^{0.47} \quad for \; \frac{\rho_N}{\rho_S}\left(\frac{U_N}{C_N}\right)^3 > 0.07$$

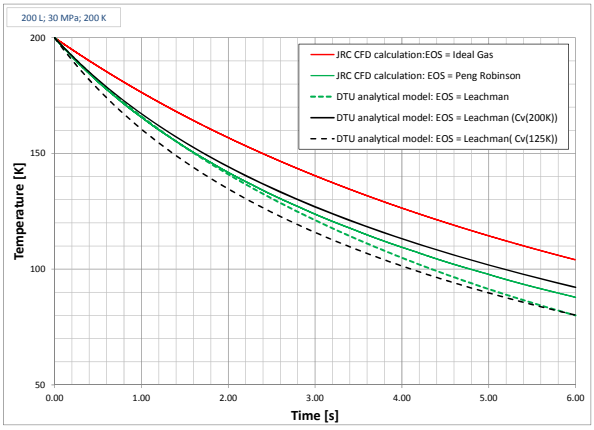

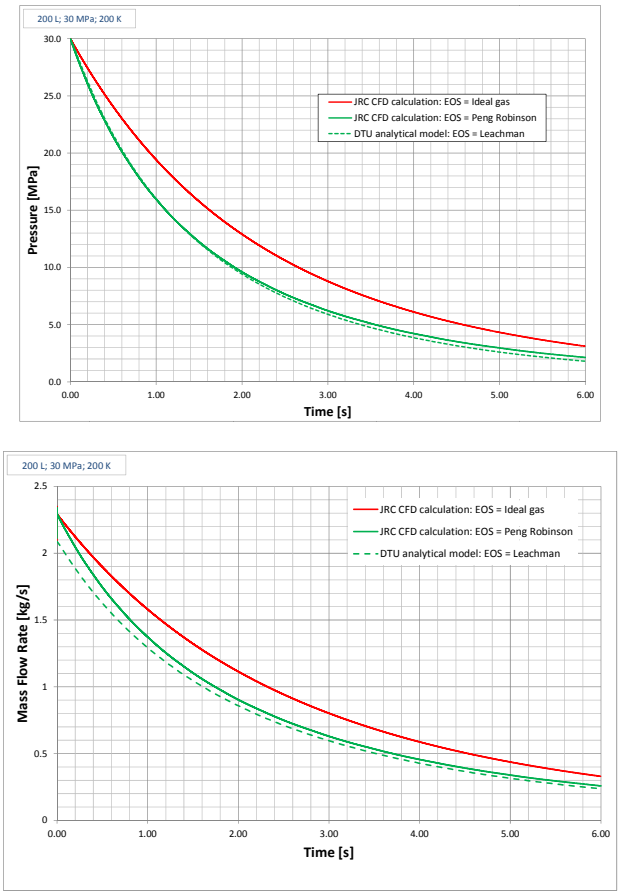

Figure 9. Results for the 197L vessel releases at 30MPa and 200K the hole size radius was 5.7mm

Where L_F is the flame length, D is the nozzle diameter, ρ_N is the density at the nozzle, ρ_S is the density of the surrounding air, U_N is the flow speed at the nozzle, and C_N is speed of sound at conditions of the gas in the nozzle. For choked flows (M=1) the dimensionless flame length depends only on the hydrogen density in the nozzle ρ_N. The density decreases with the decreasing tank pressure and therefore the maximum flame length occurs at the beginning of the release as shown in Figure 10. Since the density is overestimated with the ideal gas equation compared to the real gas equation, also the flame length is larger in the ideal case than in the real case.

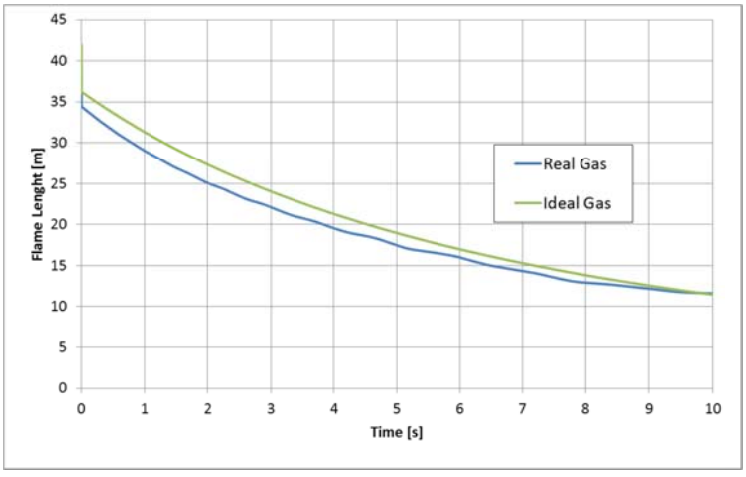

Figure 10: Flame length versus time for the 200L tank. Real gas equation used is the Peng-Robinson EOS.

An evaluation of blast effects and safety distances for unconfined hydrogen explosions can be performed using a simple approximate method that was developed by Dorofeev [11] for that purpose. The main parameter in the model is the total mass of released hydrogen and the worst case conditions of nearly instantaneous releases of hydrogen are assumed. We assume that all the hydrogen in the tank is released as a further conservative condition. Given the different initial density in the real case (26 kg/m^3) and in the ideal case (30 kg/m^3) for the 200 L tank, the total mass in the ideal case is about 6 kg while it is 5.2 in the real case. Dorofeev defines 3 different levels of congestion (high, medium and low) according to the distance between obstacles and to the size of the obstacles. He also identifies 4 levels of damages to the building: minor structural damage, serious structural damage, partial destruction (50-75%) and total destruction of buildings. If we use Dorofeev's diagrams to provide an approximate conservative indication of the safety distances for the case of high congestion in the real case, the safety distance is about 45 m for the minor structural damage, 17 m for the serious structural damage, 10 m for partial destruction (50-75%) and 7 m for total destruction of buildings. In the ideal case, those distances are about 10% longer.

5.0 CONCLUSIONS AND DISCUSSION

The paper describes a modeling approach comparing the use of an engineering numerical model and a CFD outflow model to characterize the hydrogen outflow from a pressurized vessel at ambient and cryogenic temperatures. Different EOS are used to predict the real gas behavior of hydrogen and the results are being compared focusing on the mass release rate , the time profile of the vessel pressure as well as the time profile of the vessel temperature. The models have been compared to former findings in the literature and excellent agreements for both time profiles are found at ambient conditions using the ideal gas EOS. Real gas EOS, as the reference NIST data by Leachman, the Peng Robinson, Beattie Bridgeman and the Abel Nobel EOS[6], gave also excellent agreement for the vessel pressure decays, but there are differences observed for the temperature profiles.

The DTU analytical model and the JRC CFD code are then applied to low temperature storage release scenarios at 200K and two vessel sizes. The results for the 27L and 200L vessel also show good comparison for the release rates and the pressure time profile, while some more scatter (compared to the ambient conditions) are seen in the temperature time profile of the vessel.

It seems that the results are sensitive to the chosen strategy to predict the C_v value in the models. This dependency is not seen so strongly in the ambient releases and simple constant C_v start values may be applied. For low temperatures, such simple assumptions are questionable due to the increasing non-linearity in the specific heat capacity C_v with decreasing temperatures.

Simple models have been applied to estimate the consequence of the ignition in the case of the release for the 200 L tank. The dominant parameter for the flame length is the density at the nozzle and therefore by using the ideal gas law one will overestimate the flame length compared to the estimate with the real gas equation. The strength of an explosion is related to the total amount of mass that is released and therefore to the gas density inside the tank. Since the density is larger with the ideal law than with the real law, also in the case of explosions, by using the ideal law one overestimates the consequence of the accident.

6.0 REFERENCES

1. O. Kircher, G. Greim, J. Burtscher, T. Brunner, Validation of cryo-compressed hydrogen storage (CCH2) - A probabilistic approach, (2011).
2. S.M. Aceves, F. Espinosa-Loza, E. Ledesma-Orozco, T.O. Ross, A.H. Weisberg, T.C. Brunner, O. Kircher, High-density automotive hydrogen storage with cryogenic capable pressure vessels, Int J Hydrogen Energy. 35 (2010) 1219-1226.

[6] See appendix A

3. J.W. Leachman, R.T. Jacobsen, S.G. Penoncello, E.W. Lemmon, Fundamental Equations of State for Parahydrogen, Normal Hydrogen, and Orthohydrogen, Journal of Physical and Chemical Reference Data. 38 (2009).
4. A.V. Tchouvelev, Z. Cheng, V.M. Agranat, S.V. Zhubrin, Effectiveness of small barriers as means to reduce clearance distances, International Journal of Hydrogen Energy. 32 (2007) 1409-1415.
5. R.W. Schefer, W.G. Houf, T.C. Williams, B. Bourne, J. Colton, Characterization of high-pressure, underexpanded hydrogen-jet flames, Int J Hydrogen Energy. 32 (2007) 2081-2093.
6. J. Xiao, J.R. Travis, W. Breitung, Hydrogen release from a high pressure gaseous hydrogen reservoir in case of a small leak, Int J Hydrogen Energy. 36 (2011) 2545-2554.
7. E. Papanikolaou, D. Baraldi, M. Kuznetsov, A. Venetsanos, Evaluation of notional nozzle approaches for CFD simulations of free-shear under-expanded hydrogen jets, Int J Hydrogen Energy. 37 (2012) 18563-18574.
8. J.A. Salva, E. Tapia, A. Iranzo, F.J. Pino, J. Cabrera, F. Rosa, Safety study of a hydrogen leak in a fuel cell vehicle using computational fluid dynamics, Int J Hydrogen Energy. 37 (2012) 5299-5306.
9. K. Nasrifar, Comparative study of eleven equations of state in predicting the thermodynamic properties of hydrogen, Int J Hydrogen Energy. 35 (2010) 3802-3811.
10. J.-. Saffers, V.V. Molkov, Towards hydrogen safety engineering for reacting and non-reacting hydrogen releases, J Loss Prev Process Ind. 26 (2013) 344-350.
11. S.B. Dorofeev, Evaluation of safety distances related to unconfined hydrogen explosions, International Journal of Hydrogen Energy. 32 (2007) 2118-2124.
12. Committee for the Prevention of Disasters, Methods for the calculation of physical effects due to the releases of hazardous materials (liquids and gases) 'Yellow Book', CPR 14E (1997).
13. K. Mohamed, M. Paraschivoiu, Real gas simulation of hydrogen release from a high-pressure chamber, International Journal of Hydrogen Energy. 30 (2005) 903-912.
14. R.J. Sadus, Influence of quantum effects on the high-pressure phase behavior of binary mixtures containing hydrogen, J. Phys. Chem. 96 (1992) 3855.
15. ANSYS CFX User's Guide, ANSYS Inc. (2012).
16. Pointwise User Manual. Release 17.0, Pointwise Inc. (2012).
17. E.W. Lemmon, M.L. Huber, J.W. Leachman, Revised Standardized Equation for Hydrogen Gas Densities for Fuel Consumption Applications, Journal of Research of the National Institute of Standards and Technology. 113 (2008) 341-350.
18. V. Molkov, J. Saffers, Hydrogen jet flames, Int J Hydrogen Energy. In press: http://dx.doi.org/10.1016/j.ijhydene.2012.08.106.

APPENDIX A

Table 4.numerical procedure to calculate vessel dynamics at sonic conditions

for $i \in 0..N_t$

$t_i \leftarrow \delta t \cdot i$

$$qs_i \leftarrow C_D \cdot A \cdot \psi \cdot \sqrt{\gamma \cdot \rho_i P_i \cdot \left(\frac{2}{\gamma+1}\right)^{\frac{\gamma+1}{\gamma-1}}}$$

$$\delta\rho_i \leftarrow -\frac{qs_i}{V} \cdot \delta t$$

$$\delta T_i \leftarrow \frac{P_i}{(\rho_i)^2 \cdot C_v} \cdot \delta\rho_i$$

$T_{i+1} \leftarrow T_i + \delta T_i$

$\rho_{i+1} \leftarrow \rho_i + \delta\rho_i$

$$P_{i+1} \leftarrow Z(P_i, T_{i+1}) \cdot R_{gas} \cdot \frac{T_{i+1} \cdot \rho_{i+1}}{MM}$$

$total\_m_{i+1} \leftarrow total\_m_i + qs_i \cdot \delta t$

(break) if $P_{i+1} \le 2 \cdot 10^5 Pa$

Where t_i – time, s; δt – time step, s; qs_i – mass flow rate, kg/s; C_D – discharge coefficient; A – hole area, m^2; Ψ = 1- sonic release; γ- C_p/C_v; ρ_I – density, kg m^{-3}; P_i – vessel pressure, Pa; V – vessel volume, m^3; δT_i – temperature difference, K; T_i – vessel temperature, K; C_v – isochoric specific heat capacity, J mol^{-1} K^{-1}; Z(P,T) – compressibility factor; R_{gas} – gas constant, 8.314 J mol^{-1} K^{-1}; MM – molecular weight, 0.002 kg mol^{-1}

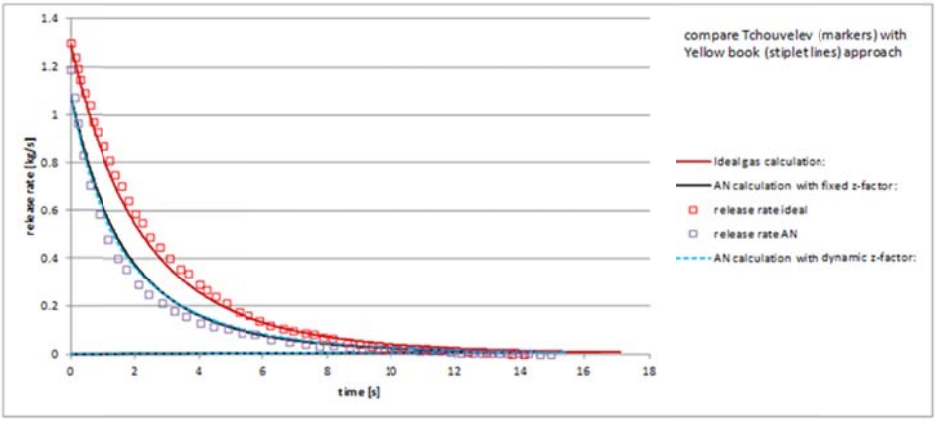

Figure 11. Figure 12Comparison of ideal and AN EOS predictions at 70MPa as published by Tchouvelev et al. [4](squares) with the yellow book model (lines).

Tchouvelev et al. [4] investigated the effects of hydrogen's real gas behaviour using computational fluid dynamics (CFD) modelling techniques. The 60L vessel was initially at 70 MPa, and an accidental hydrogen release impinging horizontally into the wall was assumed. An in-house CFD codes accurately estimated the non-linear hydrogen mass release rate decreasing with time using the PHOENICS software package, both with the ideal gas law and the real gas Abel-Nobel equation of state (AN-EOS).